

Dynamic phases in the two-dimensional underdamped driven Frenkel-Kontorova model

Jasmina Tekić

*Department of Physics, Centre for Nonlinear Studies, The Beijing-Hong Kong-Singapore Joint Centre for Nonlinear and Complex Systems (Hong Kong), Hong Kong Baptist University, Hong Kong, China,
and Theoretical Physics Department 020, "Vinča" Institute of Nuclear Sciences, 11001 Belgrade, Serbia and Montenegro, Yugoslavia*

O. M. Braun*

Institute of Physics, National Academy of Sciences of Ukraine, 03650 Kiev, Ukraine and Department of Physics, Centre for Nonlinear Studies and The Beijing-Hong Kong-Singapore Joint Centre for Nonlinear and Complex Systems (Hong Kong), Hong Kong Baptist University, Hong Kong, China

Bambi Hu

*Department of Physics, Centre for Nonlinear Studies, The Beijing-Hong Kong-Singapore Joint Centre for Nonlinear and Complex Systems (Hong Kong), Hong Kong Baptist University, Hong Kong, China,
and Department of Physics, University of Houston, Houston, Texas 77204-5005, USA*

(Received 18 August 2004; published 8 February 2005)

We study the nonlinear dc response of a two-dimensional underdamped system of interacting atoms subject to an isotropic periodic external potential with triangular symmetry. When driving force increases, the system transfers from a disorder locked state to an ordered sliding state corresponding to a moving crystal. By varying the values of the effective elastic constant, damping, and temperature, we found different scenarios and intermediate phases during the ordering transition. For a soft atomic layer, the system passes through a plastic-channel regime that appears as a steady-state regime at higher values of the damping coefficient. For high values of the effective elastic constant, when the atomic layer is stiff, the intermediate plastic phase corresponds to a traffic-jam regime with immobile islands in the sea of running atoms. At a high driving of the stiff layer, a solitonlike elastic flow of atoms has been observed.

DOI: 10.1103/PhysRevE.71.026104

PACS number(s): 05.70.Ln, 45.05.+x, 66.30.-h, 63.20.Ry

I. INTRODUCTION

A lattice of interacting particles driven over a pinning rigid substrate represents one of the most tractable models for studying the nonequilibrium behavior and dynamic phase transitions in a wide variety of condensed matter systems such as vortex lattices in superconductors [1,2], Josephson junction, charge-density waves [3], colloids [4], Wigner crystals [5], metallic dots [6,7], magnetic bubble arrays [8], and systems in tribology [9]. In numerous experimental and theoretical studies, particular interest has been focused on the behavior, motion, dynamical phases, and structure of the lattice when driving force is varied. It was found that the system dynamics depends strongly on the main model parameters such as atomic concentration, pinning strength, and geometry of the substrate.

A number of studies are devoted to *overdamped* motion of an array of (repulsively) interacting particles over a *random* (quenched) potential of the substrate, first of all because this model describes an array of vortices in a dirty type II superconductor. The main control parameter in this case is the elastic constant g of the array (or the strength of the substrate potential if the interparticle interaction is kept fixed). For a very stiff layer, $g > g_{el}$ (or a very weak pinning potential of the substrate), the array is unpinning and begins to slide as a whole at any applied dc force. For a less stiff layer, $g_{pl} < g$

$< g_{el}$, the array is pinned by the substrate and begins to move when the applied force F exceeds a threshold value F_s (known as the static frictional force in tribology). At low driving, $F \gtrsim F_s$, the motion proceeds through discharging of elastic instabilities and exhibits a stick-slip behavior. The locked-to-sliding transition is continuous (second-order) and reversible [10]. The moving array preserves its topological order and slides as an elastic manifold. This regime is described by the collective pinning theory of Larkin and Ovchinnikov [11]. The crossover value g_{pl} increases with increasing system size and eventually vanishes for an infinite system [12] (in the context of tribology, this question was also considered by Sokoloff [13]). When the driving force increases, the stick-slip regime continuously changes to a regime of smooth sliding. The low-temperature dynamics of an elastic manifold driven through random media was described by Vinokur *et al.* [14].

In the case of a soft array, $g < g_{pl}$, the system passes through three dynamical steady phases as the driving increases: the locked state at $F < F_s$, the regime of plastic flow at $F_s < F < F_g$, and finally the regime of a homogeneously sliding array. In the plastic flow regime, the array splits into trapped regions separated by channels in which the particles flow plastically [15,16]. The flow channels in an otherwise perfect pinned lattice may be described with the help of the generalized Frenkel-Kontorova model [17]. The transition between the locked state and the plastic phase is continuous (second-order) at zero temperature and smooth at $0 < T < T_m$, when the locked state corresponds to thermally acti-

*Electronic address: obraun@iop.kiev.ua

vated creep motion (T_m denotes the melting temperature of the 2D array).

The transition from the plastic phase to the sliding ordered phase, predicted by Koshelev and Vinokur [18], occurs due to a decrease of a “shaking temperature” $T_{sh} \propto 1/v$ that emerges because of fluctuations of the array during its motion over the random potential (here v is the sliding velocity). This last transition is sharp (first-order) and hysteretic [19]. According to Giamarchi and Le Doussal [20], the sliding phase corresponds to a “moving glass” phase, where the particles move along highly correlated static channels. The static structure factor demonstrates quasi-long-range translational order in the transverse direction (with a power-law decay of the peak height) but only a short-range order in the longitudinal (driving) direction, probably due to slips between neighboring moving elastic domains [21].

The two-step transition from the locked state to an ordered sliding state has been observed experimentally for superconducting flux lattices, although there is a debate whether the strongly driven ordered state corresponds to an ordered moving crystal [22] or a moving glass with smectic order [23] or both, depending on the driving force [24] and the stiffness of the array [25].

In recent years, particular interest has been focused on the dynamics of an array driven over a *periodic* substrate. These systems show a richer variety of dynamical plastic flow phases than those with a random substrate. The locked-to-sliding transition in the *overdamped* driven two-dimensional Frenkel-Kontorova (2DFK) model with different symmetries of the substrate (with the square or triangular potential) has been studied by Reichhardt *et al.* [26–29]. Now the behavior of the driven system depends first of all on the dimensionless concentration θ (the so-called coverage), which is defined as the ratio of the number of atoms to the number of minima of the substrate potential.

In the commensurate case, when θ is a rational number, the critical depinning force is larger than in the incommensurate case, and the locked-to-sliding transition occurs in one step. This was shown, in particular, for the concentrations $\theta=1, 6/7, 2/3, 1/3, 1/4, 1/6$, and $1/7$ driven over the triangular substrate, where the locked phase has an ordered structure achieved after annealing an initial random configuration, while the sliding phase corresponds to the moving crystal (the “elastic flow” phase) [27].

For an incommensurate coverage, when the annealed locked state is typically disordered [27], the locked-to-sliding transition proceeds through several plastic flow phases [26,28]. These phases depend strongly on the substrate geometry and result from the interaction of the interstitial atoms with the atoms at the commensurate positions. In spite of their complexity, two general types of flow can be identified: an elastic flow (a stable channel flow) of the sublattice of interstitial atoms and a chaotic or mixing flow when the motion of interstitial atoms is disordered. The transitions between these phases exhibit a hysteretic behavior and are characterized by jumps (dips) in the $v(F)$ dependence. At a low concentration, $\theta < 1$, first vacancies or interstitial defects depin and move in one-dimensional channels; this corresponds to the plastic flow phase. Then with the increase of driving, the whole lattice starts to move, under-

going an ordering transition from the plastic regime to the elastic distorted triangular moving lattice [27].

For a high concentration, $\theta > 1$, Reichhardt *et al.* [26] observed for the square substrate potential the following sequence of phases during the force increasing process: (i) the pinned phase; (ii) the phase where interstitial atoms begin to move between the pinned atomic rows; (iii) the motion of interstitial atoms becomes chaotic, and the pinned atoms begin to take part in the motion too, with any atom moving for a time and then being trapped again; (iv) the phase with ordered solitonlike one-dimensional flow due to kinks (local compressions) moving along the pinning channels; and, finally, (v) the sliding crystal phase. A similar and even more rich behavior exhibits an array driven over the rectangular substrate [28].

An interesting phenomenon has also been found when the direction of driving was varied [30]. For example, for certain directions of the driving, a spontaneous symmetry breaking was observed for the overdamped system of repulsively interacting atoms on the triangular substrate. The atomic flow is not in the direction that is aligned with the external force but in one of the symmetry directions of the substrate. In the case of a square lattice, the change of the force direction can produce the series of dynamical mode-locking phases which forms the devil’s-staircase structure [31].

Contrary to a large number of studies of the overdamped 2DFK model at zero temperature, a relatively small number of papers is dedicated to driven *underdamped* systems, especially at nonzero temperatures. The main new issue of the underdamped system is *bistability*: now an atom may possess a running state even before the minima of the total potential vanish because the momentum of the atom can help it to overcome the barriers. The behavior of the underdamped system is strongly affected by one more model parameter, the damping coefficient η in Langevin equations, which describes the rate of energy exchange between the moving array and the substrate.

The locked-to-sliding transition in the one-dimensional FK model has been studied in a series of papers [32–36]. It was shown that the transition to the running state occurs due to *dynamical instability* of topological excitations (kinks) at high velocities [33,37,38]. A similar behavior exhibits the anisotropic 2DFK model, which may be treated as a system of weakly coupled 1DFK chains. As for the *isotropic* 2DFK model, it was studied for highly commensurate concentrations only [39]. For a closely packed layer of $\theta=1$ with a low elastic constant, the transition to the sliding state is achieved via the creation of an avalanche of moving particles that leaves a depleted region in its wake, while for a stiff layer, an island of moving particles nucleates the transition. In the case of a half-filled layer, $\theta=1/2$, the scenario is more subtle. Several dynamical phase transitions between states with different atomic mobility were observed, and the mobility of atoms as a function of the external force can vary nonmonotonically with increasing force.

The aim of the present work is a detailed study of the locked-to-sliding transition in the underdamped isotropic 2DFK model with the triangular substrate potential for a partially filled layer with $\theta \sim 0.75$, when the 1DFK system demonstrates the highest mobility [40]. We will show that in

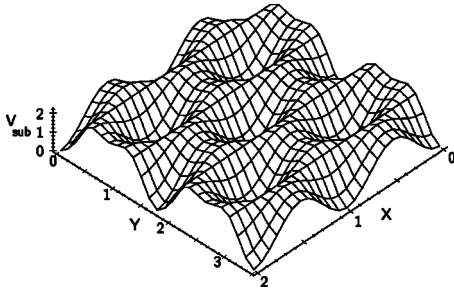


FIG. 1. The substrate potential with triangular symmetry, V_{sub} , plotted for $\varepsilon=2$. The coordinates are scaled so that $X=x/a$ and $Y=y/a$.

the underdamped system, the scenario of the locked-to-sliding transition strongly depends on the value of the damping coefficient. On the contrary, with an overdamped system where elastic flow appears for the commensurate case or for the structures with an ordered locked state, in an underdamped system even in an incommensurate disordered locked state the system transfers to the sliding state of a moving crystal at high driving forces. The plastic flow regime, commonly observed in overdamped systems, now may disappear or may exist as a transient state only. Novel phases may emerge for some range of model parameters, such as a disordered flow of atoms among the areas of immobile ones for a soft layer, or solitonic phases for a stiff layer. Finally, our simulation shows that the sliding state in the underdamped system always corresponds to a crystalline configuration. These results are especially important for tribological systems, where the mechanism of the locked-to-sliding transition determines frictional properties of a lubricant film [9,41,42].

The paper is organized as follows. The model is introduced in Sec. II. Simulation results are presented in Sec. III. Finally, Sec. IV concludes the paper.

II. MODEL

We consider a two-dimensional (2D) layer of particles with position vector $\mathbf{u}=(u_x, u_y)$ subjected to a periodic substrate potential with the triangular symmetry as a generic example of isotropic 2D systems. The substrate potential is chosen in the simplest form,

$$V_{\text{sub}}(x, y) = \frac{1}{2} \varepsilon \left\{ 1 - \cos(2\pi x/a_x) \cos(\pi y/a_y) + \frac{1}{2} [1 - \cos(2\pi y/a_y)] \right\}, \quad (1)$$

where $a_x=a$ and $a_y=a\sqrt{3}/2$ are the lattice constants. The function (1) is characterized by the isotropic minima organized into the triangular lattice and separated by isotropic energy barriers of height ε , as shown in Fig. 1. The frequencies of atomic vibrations at the minima are isotropic, $\omega_x = \omega_y = \omega_s \equiv (\varepsilon/2m)^{1/2}(2\pi/a)$. Flat maxima of the potential (1) are organized into a honeycomb lattice.

We consider the case of an exponential interaction between the atoms,

$$V(r) = V_0 \exp(-\gamma r), \quad (2)$$

where γ^{-1} is the radius of interaction. The repulsive interaction corresponds, for example, to atoms chemically adsorbed on a metal surface when, due to breaking of the translation symmetry in the direction normal to the surface, the atoms have a nonzero dipole moment which leads to their mutual repulsion [43]. In the simulation we chose $\gamma=a^{-1}$, so that the interaction is short-ranged.

One of the main parameters of FK-type models is the effective elastic constant $g_{\text{eff}}=a^2 V''(r_0)/2\pi^2 \varepsilon$, where r_0 is the average interatomic distance [32]. This single dimensionless number gives an indication of the strength of the elastic constant of the atomic layer relative to the strength of the substrate potential. A value of g_{eff} much smaller than 1 indicates a relatively weakly coupled layer. This situation may correspond, for example, to a monolayer adsorbed on a crystal surface. A value $g_{\text{eff}} \gtrsim 1$ describes a stiff atomic layer compared with the substrate depth. For example, the case of dry friction between two blocks of material corresponds to this limit.

The equation of motion for the displacement vector \mathbf{u}_i ($1 \leq i \leq N$) is given by the Langevin equation,

$$\ddot{w}_i + \eta \dot{w}_i + \frac{d}{dw_i} \left[\sum_{j(j \neq i)} V(|\mathbf{u}_i - \mathbf{u}_j|) + V_{\text{sub}} \right] = F^w + F_{\text{rand}}^w, \quad (3)$$

where $w=u_x$ or u_y . We use dimensionless system of units, where the atomic mass is $m=1$, the periodicity of the substrate potential is $a=2\pi$, and its height is $\varepsilon=2$, so that the characteristic frequency is $\omega_s=1$. The time scale that we use in the problem is defined in terms of the oscillation period of a particle in the substrate potential, $\tau_s=2\pi$. The time scale could also be defined in terms of the oscillation period of an atom in the layer, $\tau_0=\tau_s/\sqrt{g_{\text{eff}}}$. The force $F^w=F^x$ or F^y is the externally applied force, while F_{rand}^w is the random force required to equilibrate the damped system to a given temperature T . In the present work, we consider a driving force acting in the x direction only, so that $F^x=F$ and $F^y=0$.

The damping coefficient η strongly determines the dynamics of the system [32–40]. For a small applied force F , the total potential experienced by a particle possesses an array of local minima. Hence the particles are in the locked state and the system mobility $B=\langle v \rangle/F$ vanishes at zero temperature and is exponentially small at low temperatures (here v is the drift velocity). When F increases, the system will behave in different ways depending on the value of the damping coefficient. In the overdamped case, $\eta \gtrsim \omega_s$, at some critical force F_c the minima in the total potential vanish and the particle begins to slide over the corrugated total potential with a maximum mobility of $B=(m\eta)^{-1}$ so that the system is in the sliding state. In the underdamped case, $\eta \ll \omega_s$, the system may possess a sliding solution even before the minima of the total potential vanish.

The numerical procedure used for solving the equations was the same as in our previous works [33–35]. The atoms were first thermalized at zero force; then the force was adiabatically increased with the step $\Delta F=0.005$, allowing a time

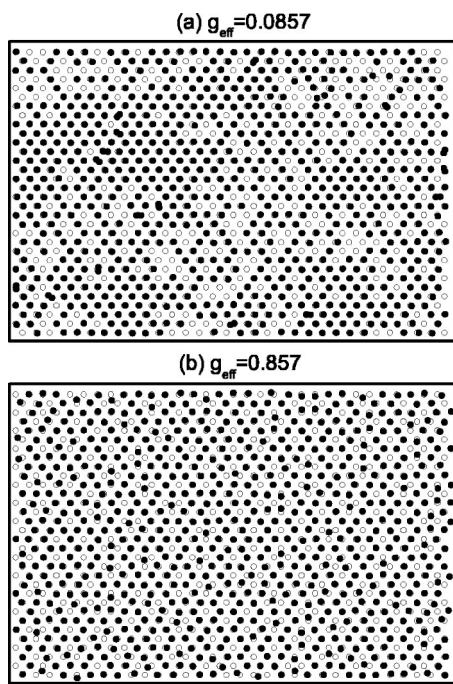


FIG. 2. Locked state of the system for the concentration $\theta = 3/4$ at $T=0.001$ for two values of the effective elastic constant: (a) $g_{\text{eff}}=0.0857$ and (b) $g_{\text{eff}}=0.857$. Atoms are indicated by black dots and pinning sites by open circles.

of several hundreds of τ_s (or τ_0 if $\tau_0 > \tau_s$) to equilibrate at each new value of force where the equilibrated configuration of positions and velocities was stored, allowing one to restart the simulation with a finer force step. In this way, the force was increased until one had moved through the transition. Once the transition had been located for the given system parameters, the atomic trajectories were examined with the help of the visual molecular dynamics (VMD) technique [44] to allow the identification of the scenario for the transition.

III. RESULTS

We modeled the atomic layer by $N=768$ atoms placed randomly onto the triangular substrate of size $M=M_x M_y = 32 \times 32 = 1024$, so that the dimensionless concentration is $\theta=3/4$. The random initial configuration was then annealed. We analyzed the locked-to-sliding transition for different values of the elastic constant g_{eff} ($g_{\text{eff}}=0.0857, 0.257$, and 0.857), the damping coefficient η ($\eta=0.1, 0.3$, and 1), and two choices of the temperature ($T=0.001$ and 0.1). All quantities that we use are dimensionless.

Figure 2 shows typical atomic configurations at the locked state for two values of g_{eff} .

When the interatomic interaction is weak, as, e.g., for the $g_{\text{eff}}=0.0857$ case shown in Fig. 2(a), almost all atoms lie at the substrate minima. Among the areas with the perfect triangular structure, there are regions with vacancies and a small number of interstitial atoms. The interstitial atoms lie at positions between the pinning sites, where they are trapped due to the repulsion of interstitial atoms with those at the pinning sites. These interstitial atoms play a key role in

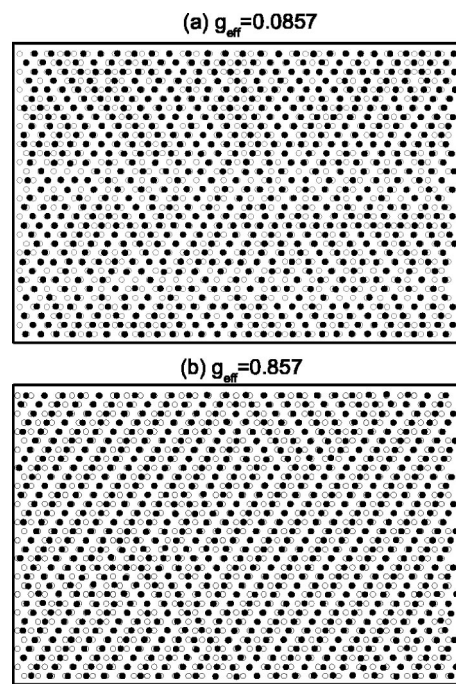


FIG. 3. Crystalline structure of the sliding state for $\theta=3/4$, $\eta = 0.1$, and $T=0.001$ at $F=0.8$ for two values of the effective elastic constant: (a) $g_{\text{eff}}=0.0857$ and (b) $g_{\text{eff}}=0.857$. Atoms are indicated by black dots and pinning sites by open circles.

the scenario of the locked-to-sliding transition, because they are the first ones that start to move and initiate the transition of the whole layer to the sliding state.

For higher values of the elastic constant, e.g., for $g_{\text{eff}}=0.857$ shown in Fig. 2(b), the structure of the locked state is more homogeneous, since due to the stronger interatomic interaction with respect to the substrate potential, the atoms may adjust their mutual positions by taking interstitial sites.

At high driving force the system is in the sliding state and takes an ordered homogeneous configuration as shown in Fig. 3. In both cases of the weak or stiff layer, the sliding phase forms a moving crystal which consists of ordered domains and dislocation lines between them. When the interatomic interaction is stronger, the crystalline structure is more ordered. For example, for the $g_{\text{eff}}=0.857$ case shown in Fig. 3(b), one can clearly distinguish large ordered domains of different orientations.

For the underdamped system we always observed a transition from a disordered locked state to an ordered sliding state of a moving crystal. This is clearly seen from Fig. 4, where we plot the static structure factor

$$S(\mathbf{k}) = A^{-1} \left\langle \sum_{ij} \exp\{i\mathbf{k} \cdot [\mathbf{u}_i(t) - \mathbf{u}_j(t)]\} \right\rangle, \quad (4)$$

where A is the area of the system and $\langle \dots \rangle$ stands for averaging over time.

As we can see, in both cases $S(k)$ changes significantly in the sliding state. Although the appearance of two peaks at large k_y in Fig. 4(c) may be considered as an indication of a smectic order, in the VMD simulation we have clearly observed the crystalline flow [45].

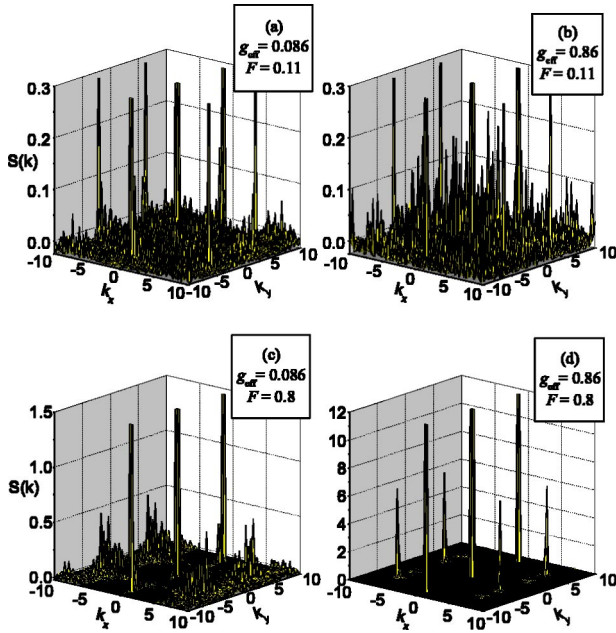


FIG. 4. (Color online) Structure factor for the soft ($g_{\text{eff}}=0.0875$) and stiff ($g_{\text{eff}}=0.857$) layers for $\eta=0.1$ and $T=0.001$ at two values of the force: (a) and (b) for $F=0.11$ (the locked state, see the configurations in Fig. 2), and (c) and (d) for $F=0.8$ (the sliding state, see the configurations in Fig. 3).

However, the scenario of the locked-to-sliding transition and the intermediate phases through which the lattice passes during the ordering transition are strongly determined by the values of g_{eff} , η , and T . In the simulations, we observed several phases that we define as follows.

(i) *The locked phase* of immobile particles that is disordered and with homogeneity that increases with g_{eff} .

(ii) *The plastic phase*, where different portions of the lattice are moving with different velocities, or some are moving while others remain pinned. The plastic phase can be in the form of immobile regions in the sea of running atoms that we call the “traffic-jam” (TJ) plastic phase, or in the form of channels that we call the plastic channel phase. In the TJ plastic phase all particles are mobile, but at any moment a subset of particles spends some short time pinned and then continues to move again. In the VMD simulations, these pinned regions appear as entities that migrate in the direction opposite to the driving force. On the contrary, with the TJ plastic phase where all particles participate in the motion, in the plastic channel phase only one part of the particles is mobile while the other remains pinned for an extremely long time. In the simulation, one can observe the channels of crystalline or disorder flow separated by a channel of immobile particles. For some values of the system parameters, the channels of crystalline flow separated by the channels of disorder or TJ flow can also appear, but by changing the frame of reference one can go back again to the channels of mobile and immobile particles.

(iii) *The solitonic phase*, where the motion of particles inside the row is not continuous but in the kink like or pulse-like fashion.

(iv) *The moving crystal* that represents an ordered homogeneous sliding phase.

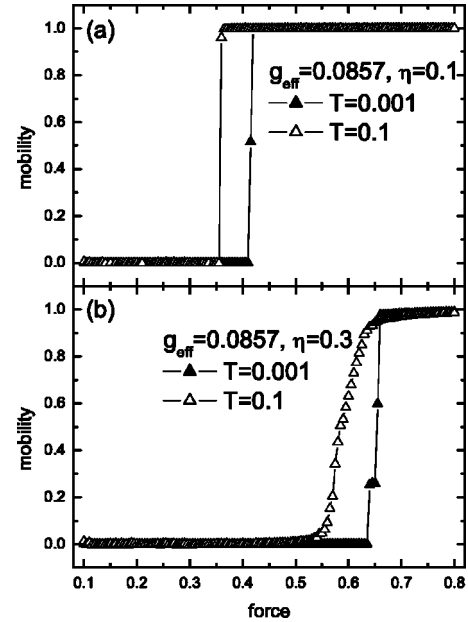


FIG. 5. The mobility B as a function of driving force for $\theta=3/4$ for the soft layer with $g_{\text{eff}}=0.0857$ and two values of damping coefficient: (a) $\eta=0.1$ and (b) $\eta=0.3$ at low temperature $T=0.001$ (solid triangles) and at high temperature $T=0.1$ (open triangles).

A. Ordering transition of the weakly bound layer

Figure 5 presents the $B(F)$ dependencies for the weak interatomic interaction $g_{\text{eff}}=0.0857$ and two values of damping $\eta=0.1$ and 0.3 at low and high temperature. We observed several intermediate phases during the locked-to-sliding transition.

As the force increases, at the low temperature $T=0.001$, the system undergoes a sharp transition from the disordered pinned phase to the moving crystal phase. In the case of low damping, $\eta=0.1$ [see Fig. 5(a)], the system transfers directly from the locked state to the sliding state without any intermediate steady-state regimes. At the fixed value of force that corresponds to the critical value $F_c \approx 0.415$, we observed the whole process of transition during the time interval of our simulations. The atomic motion starts first in the regions with vacancies while the rest of the lattice is immobile [45]. The mobile regions grow and spread mainly in the direction of driving force forming channels with very disordered flow of particles in the driving direction. This stage represents a typical example of plastic phase with channels of disordered flow separated by the regions (channels) of immobile particles. Further, the moving channels broaden in the y direction. During this process, the atomic structure inside the moving regions becomes more and more crystalline. The ordering starts first at the middle of a moving channel and then broadens in the y direction. At the same time the particles in the immobile channels begin to move chaotically. At the next stage of the plastic phase we observed a channel of ordered elastic (crystalline) flow and a channel with disordered flow of particles. With a further increase of time, the ordering spreads over the whole lattice and the system reaches the sliding state of a moving crystal. The whole lattice flows elastically and its structure is preserved during motion.

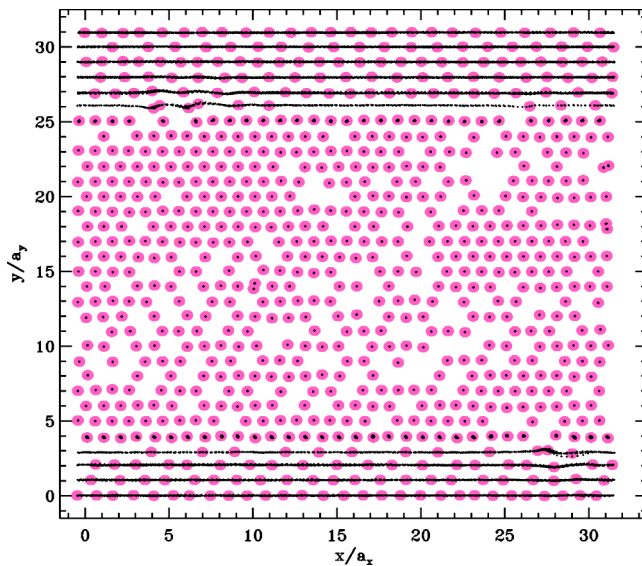


FIG. 6. (Color online) Snapshot configuration of the plastic channel phase at $F=0.645$ for $g_{\text{eff}}=0.0857$, $\eta=0.3$, and $T=0.001$. Solid curves show atomic trajectories. The channel of moving atoms is separated by the wide region of immobile atoms (the middle part of the figure).

At the high temperature $T=0.1$, due to thermal fluctuations the locked-to-sliding transition starts at a lower value of the depinning force as one can see from Fig. 5(a). While in the low- T case the atoms in the locked state were immobile, at the high temperature the drift of atoms starts in the sea of thermally fluctuating particles. Then the scenario is similar to that of the low-temperature case. The moving regions appear at places with a lower concentration of atoms, where vacancies allow the atoms to move in the driving direction. Then a river of running atoms is formed, and its width grows. Finally, the system transfers to the crystalline sliding state, passing through the plastic phase.

For a higher value of the damping coefficient $\eta=0.3$ [see Fig. 5(b)], the scenario of the transition is in general very similar to that of the $\eta=0.1$ case. Now the transition starts at a higher value of the force. When the force increases at the low temperature $T=0.001$, the system again transfers first to the plastic phase before it reaches the crystalline sliding state. However, contrary to the previous case of $\eta=0.1$, now the plastic flow appears as a truly steady state. The $B(F)$ dependence shown in Fig. 5(b) demonstrates a narrow step (only three points) at $F \approx 0.64$. This step corresponds to the plastic phase that in the time interval of our simulation appeared as a steady state [45]. The atomic structure in this state is shown in Fig. 6.

One can see a stationary channel of running particles (strips at the top and bottom of the figure; recall that we use periodic boundary conditions) separated by the channel of immobile atoms (wide region at the middle of figure). The distribution of atomic velocities $P(|v|)$ for different values of the local density ρ is shown in Fig. 7 as a three-dimensional map. The distribution has two well-separated peaks, one corresponding to sliding atoms and another to immobile atoms. Also, this figure shows that immobile regions are characterized by a slightly higher local concentration of atoms.

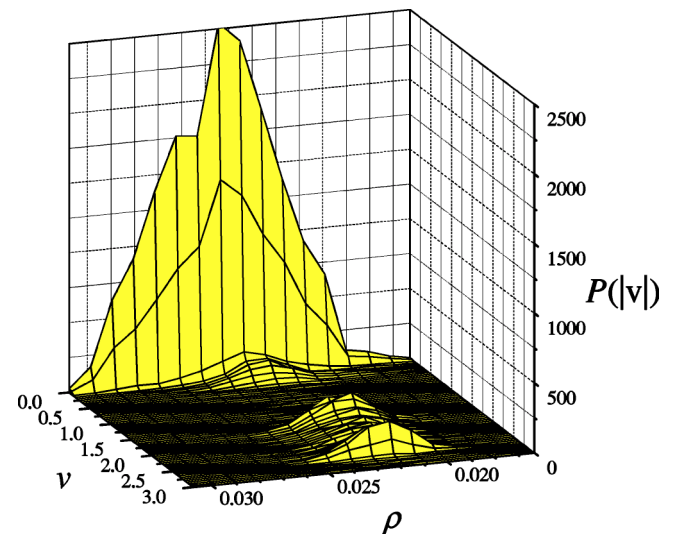


FIG. 7. (Color online) Distribution of atomic velocities $P(|v|)$ for different values of the local density ρ (calculated as an average over a circle of radius $3a$) for the system parameters $g_{\text{eff}}=0.0857$, $\eta=0.3$, and $T=0.001$ in the plastic channel regime at the force $F=0.645$ for the configuration of Fig. 6.

Finally, at large driving the system transfers to the crystalline sliding phase.

At the high temperature $T=0.1$, the plateau on the $B(F)$ dependence with a channel-like plastic steady state is destroyed. The locked-to-sliding transition is smooth as shown in Fig. 5(b). On increasing the driving force, the particles first start to move chaotically in the regions with vacancies. Among the areas with chaotic motion, there are immobile islands with thermally fluctuating particles [45]. As one can see from Fig. 8, the immobile islands resemble two-dimensional “traffic jams” (TJ’s) in the sea of running atoms. Note that a local concentration in the running regions is lower than in the regions of TJ’s.

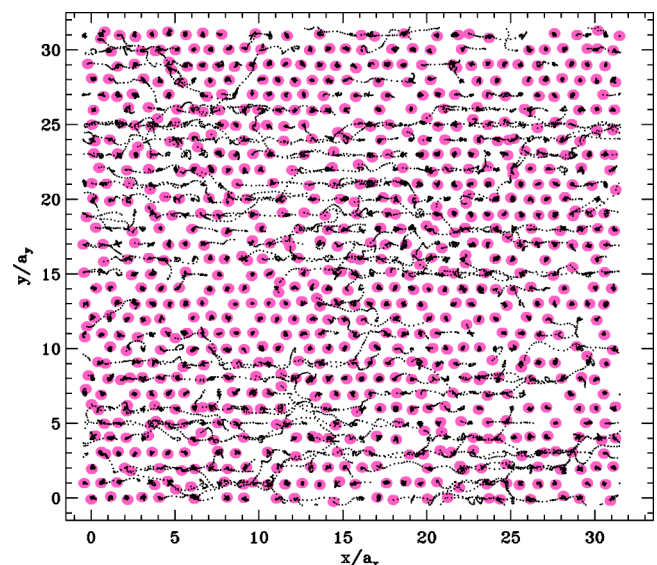


FIG. 8. (Color online) Snapshot configuration of the TJ plastic phase at $F=0.57$ for $g_{\text{eff}}=0.0857$, $\eta=0.3$, and $T=0.1$, when $B \approx 0.2$. Solid curves show atomic trajectories.

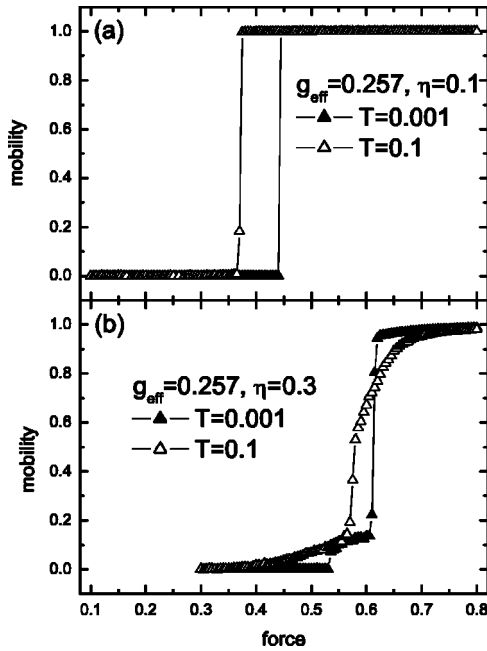


FIG. 9. The mobility B as a function of driving force for $\theta = 3/4$, $g_{\text{eff}}=0.257$, and two values of damping coefficient: (a) $\eta = 0.1$ and (b) $\eta = 0.3$ at $T=0.001$ (solid triangles) and $T=0.1$ (open triangles).

As the force increases, the areas with disordered motion spread over the whole lattice, and we observe a very disordered flow of particles in the driving direction. At a higher driving force, the process of ordering begins, and the disordered flow transforms into the sliding crystalline phase.

If we increase the stiffness of the layer to the value $g_{\text{eff}}=0.257$, the scenario of the locked-to-sliding transition remains essentially the same, as one can see from Fig. 9.

For the case of low damping, $\eta=0.1$, the only difference from the $g_{\text{eff}}=0.0857$ case is in the structure of channels at the low temperature: now we observed a formation of four channels, two channels of moving atoms separated by two channels of immobile particles. For the case of $\eta=0.3$ at the low temperature [see Fig. 9(b)], a new intermediate disordered phase emerges at the beginning of the transition prior to the plastic steady state with channel flow. At $F \approx 0.54$, the mobility increases to the value $B \approx 0.12$ and remains approximately constant with further increase of the force. This plateau corresponds to a disordered flow of particles among the areas of the immobile ones [45], which again is reminiscent of the TJ regime (see Fig. 10).

As the force increases further, the disorder phase transforms into the plastic-channel one at $F \approx 0.615$, which appears again as a steady state, at least in the time interval of our simulation. At this value of the force, we observed two moving channels [45], one wider channel of elastically moving particles and another channel with slower moving and less ordered atoms as shown in Fig. 11.

Finally, at $F=0.62$ the system transfers to the state of a sliding crystal. For the case of $\eta=0.3$ and the high temperature $T=0.1$, the channel-flow regime is absent, and the locked-to-sliding transition proceeds through the TJ plastic flow regime.

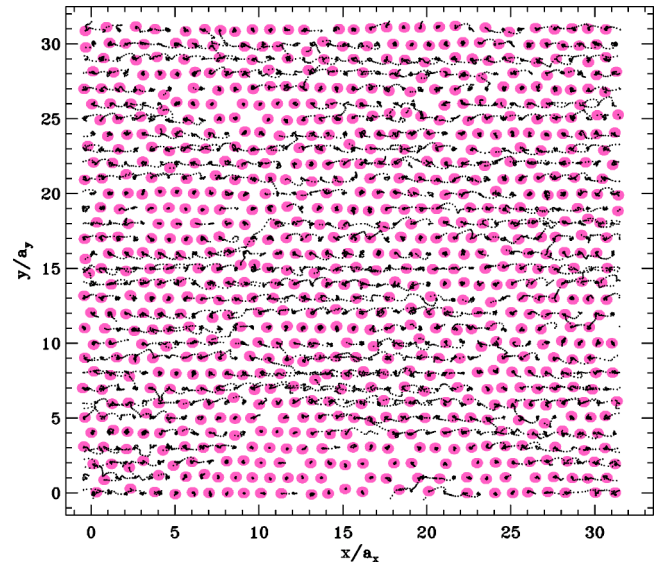


FIG. 10. (Color online) Snapshot configuration of the TJ plastic phase at $F=0.6$ for $g_{\text{eff}}=0.257$, $\eta=0.3$, and $T=0.001$. Solid curves show atomic trajectories.

B. Ordering transition of the stiff layer

The mobility as a function of the driving force for the stiff layer with $g_{\text{eff}}=0.857$ for two values of damping coefficient is presented in Fig. 12.

Starting from the locked phase, we observed a disordering of structure when the driving force increases. For the low damping $\eta=0.1$ at the low temperature $T=0.001$ [see Fig. 12(a)], an intermediate phase appears at $F \approx 0.12$ when the system goes from the pinned state to the disordered steady state with low mobility $B \sim 0.1$. At this phase, the atoms move chaotically around their pinning sites. Looking at atomic trajectories (see Fig. 13), we may suggest that this state again corresponds to a TJ plastic regime with immobile

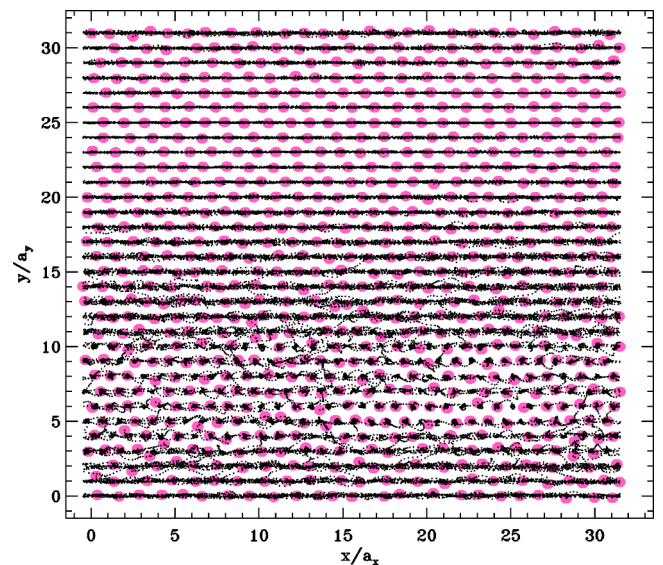


FIG. 11. (Color online) Snapshot configuration of the channel plastic phase at $F=0.615$ for $g_{\text{eff}}=0.257$, $\eta=0.3$, and $T=0.001$. Solid curves show atomic trajectories.

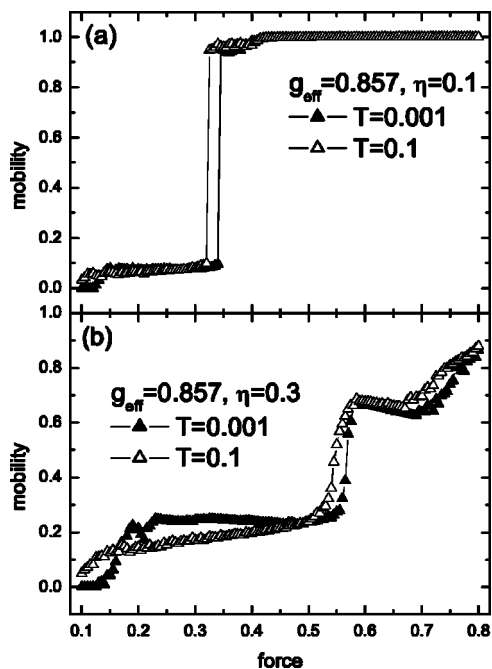


FIG. 12. The mobility B as a function of driving force for $\theta = 3/4$, $g_{\text{eff}}=0.857$, and two values of damping coefficient: (a) $\eta = 0.1$ and (b) $\eta = 0.3$ at $T=0.001$ (solid triangles) and $T=0.1$ (open triangles).

islands surrounded by regions of slowly running atoms [45]. Unfortunately, we were unable to study these TJ regimes in detail because of the too small size of our system.

The TJ disordered steady state survives until the driving force $F \approx 0.34$. Then the mobility increases and the system transfers to the ordered state of a moving crystal, passing through the plastic-channel regime. Contrary to the case of a soft system, in the stiff system the atomic motion in the rows is arranged in a solitonlike (pulse) fashion [45]. The structure of sliding atoms for the stiff layer is shown in Fig. 14(b), where the occurrence of a kink (indicated by an arrow) is clearly seen. For comparison, Fig. 14(a) [obtained by enlarging Fig. 3(a)] shows the rows of sliding atoms for the soft atomic layer.

For a larger damping $\eta = 0.3$, the first plateau at $B \approx 0.25$ for $0.23 < F < 0.54$ again corresponds to the plastic TJ flow, but now atomic motion is essentially one-dimensional along the channels in the driving direction [45]. The moving atoms strongly oscillate in the transverse direction but remain within their rows (see Fig. 15).

The motion inside each row is similar to the 1D TJ motion in the anharmonic 1D FK model [36]: inside a row, the system splits into closely packed immobile 1D islands (traffic jams) and less dense running domains. We observed that the less mobile regions are again characterized by a higher local concentration of atoms (see Fig. 16).

As the driving force increases and reaches the value $F \approx 0.6$, the system continuously transfers to the next metastable state with $B \approx 0.65$ [the second well-defined plateau on the $B(F)$ dependence]. The atomic structure of sliding rows at the second plateau is shown in Fig. 14(c). With the help of the VMD technique, we observed at this stage a formation of moving antikinks (local expansions) in each row. These an-

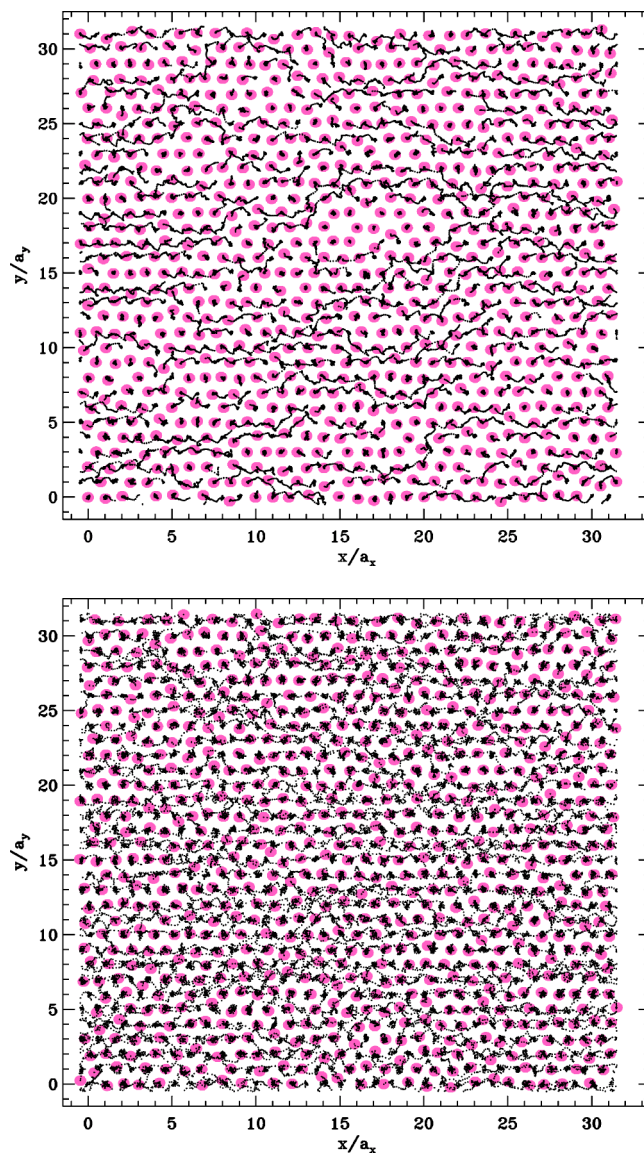


FIG. 13. (Color online) Snapshot configurations of the TJ plastic phase for $g_{\text{eff}}=0.857$, $\eta=0.1$, and $T=0.001$ at $F=0.165$ (top panel) and $F=0.33$ (bottom panel). Solid curves show atomic trajectories.

tikinks form domain walls oriented in the y direction which move in the opposite x direction [45]. With a further increase of the force, the system becomes more and more ordered and corresponds to elastic (crystalline) flow of particles.

At the higher temperature $T=0.1$, when the transition starts from the state of thermally fluctuating particles, the scenario remains approximately the same, because the melting temperature of the stiff system is much higher.

C. Overdamped system

Also we studied the locked-to-sliding transition for the case of the high value of damping coefficient $\eta=1$, when the system is overdamped.

In the case of a soft atomic layer that is equivalent to the case of strong pinning, the system never reaches the sliding state for forces $F \leq 1$. Due to the mutual action of strong

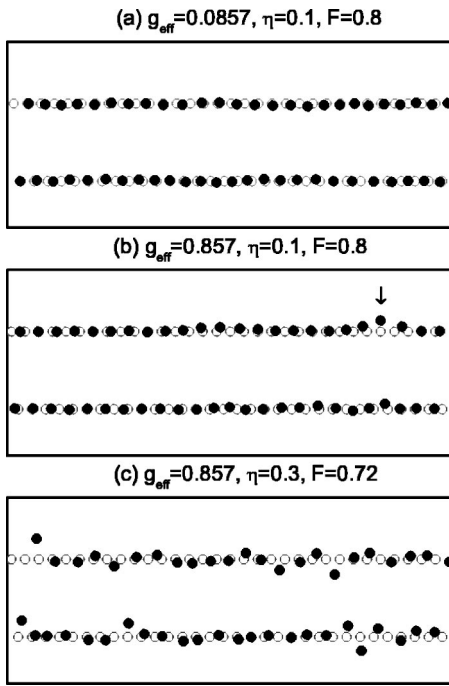


FIG. 14. The two neighboring rows of sliding atoms at $T = 0.001$ for (a) $g_{\text{eff}}=0.0857$, $\eta=0.1$, (b) $g_{\text{eff}}=0.857$, $\eta=0.1$ (an arrow indicates a position of the kink), and (c) the rows of sliding atoms in the intermediate regime at $F=0.72$ for $g_{\text{eff}}=0.857$ and $\eta = 0.3$. Atoms are indicated by black dots and pinning sites by open circles.

pinning and high damping even at high driving force $F \approx 0.8$ and high temperature $T=0.1$, the mobility of the system remains quite low, $B < 0.4$.

For the stiff atomic layer when $g_{\text{eff}}=0.857$ at $T=0.001$, we observed the appearance of a plateau at $F \approx 0.25$ with $B \approx 0.35$ that corresponds to the TJ plastic flow.

As we can see from Fig. 17, with a further increase of the force, the system remains in that phase with only a very slow

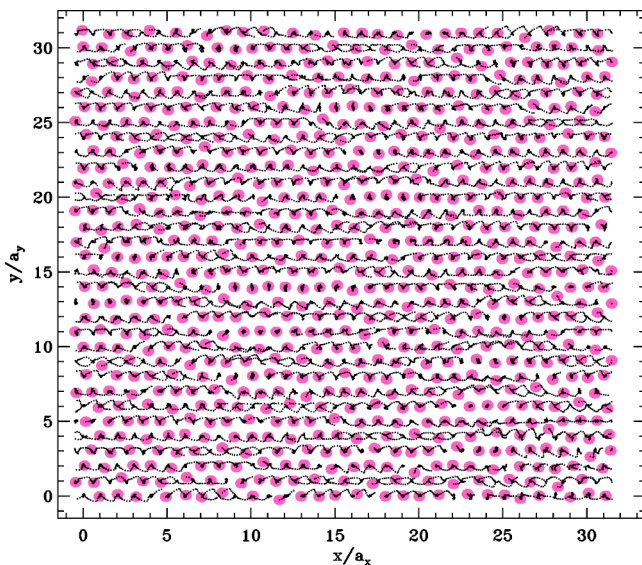


FIG. 15. (Color online) Snapshot configurations of the 1D TJ plastic phase for $g_{\text{eff}}=0.857$, $\eta=0.3$, and $T=0.001$ at $F=0.4$. Solid curves show atomic trajectories.

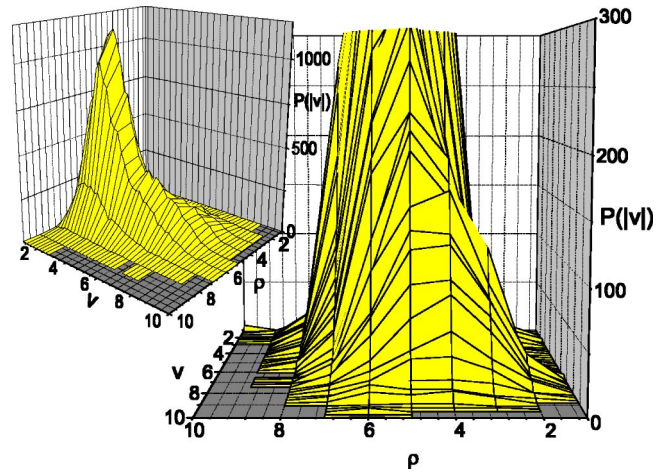


FIG. 16. (Color online) Distribution of atomic velocities $P(|v|)$ for different values of the local density ρ (calculated as an average over a circle of radius $3a$) for $g_{\text{eff}}=0.857$, $\eta=0.3$, and $T=0.001$ in the plastic flow regime at the force $F=0.4$ for the configuration of Fig. 15. The inset shows the same figure from a different perspective.

increase of the mobility at higher driving. Even at the high driving, when in all previous cases we observed the transition to the state of a moving crystal, now we found a typical TJ plastic phase with very slow flow of particles around the islands of the immobile ones. This could be seen from the plot of the static structure factor at maximum driving force $F=0.8$ in Fig. 18.

At the high temperature, the situation remains generally the same. When the driving force increases, the system transfers from the sea of thermally oscillating particles to the TJ plastic phase with continuously increasing mobility. These results are in very good agreement with the results of Reichardt *et al.* [26,27], where a detailed study of the locked-to-sliding transition for overdamped systems with the concentrations $\theta < 1$ was presented. For the triangular substrate, the system depins elastically for the commensurate atomic concentrations $\theta = 1, 6/7, 2/3, 1/3, 1/4$, and $1/7$, while for the incommensurate case the motion is plastic.

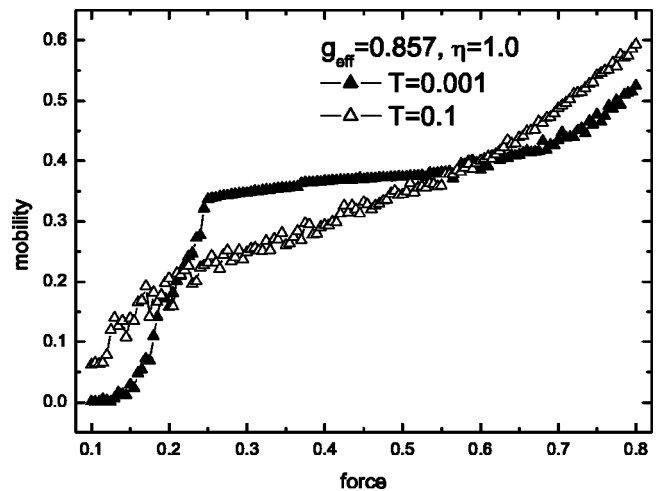


FIG. 17. The mobility B as a function of driving force for $\theta = 3/4$, $g_{\text{eff}}=0.857$, and $\eta=1$ at $T=0.001$ (solid triangles) and $T = 0.1$ (open triangles).

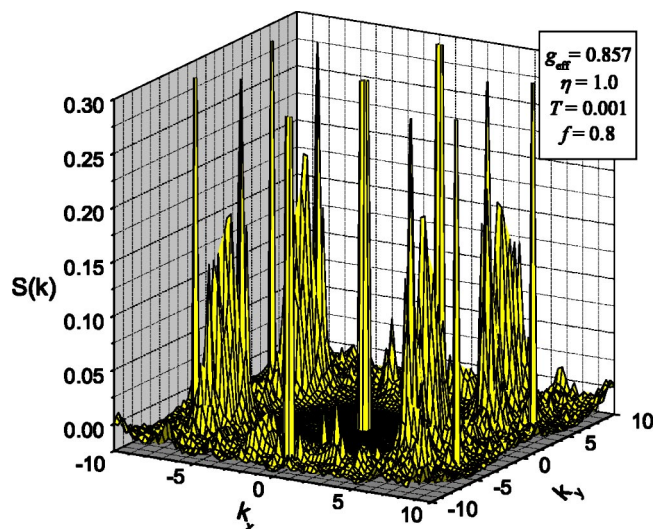


FIG. 18. (Color online) Structure factor for the overdamped stiff layer ($g_{\text{eff}}=0.857$) for $\eta=1$ and $T=0.001$ at $F=0.8$.

IV. CONCLUSION

We have presented a detailed numerical study of the locked-to-sliding transition in the underdamped isotropic two-dimensional Frenkel-Kontorova model with a triangular substrate potential for a nontrivial ground state $\theta=3/4$. Our results show that the system parameters, particularly the damping coefficient, play a crucial role in the scenario of the locked-to-sliding transition and determination of the structure of the sliding state.

When the driving force increases, the underdamped isotropic system always transfers from a disorder locked state to an ordered sliding state of a moving crystal. The scenario and the intermediate phases passing during the ordering transition strongly depend on the values of the system parameters such as the effective elastic constant, damping coefficient, and temperature. We found that the following distinctive dynamical phases could be present during the process of the locked-to-sliding transition: (i) the locked phase, (ii) the disorder TJ plastic phase, (iii) the plastic channel flow, (iv) the solitonic phase, and (v) the sliding state of a moving crystal.

For the weakly bound layer, $g_{\text{eff}}=0.0857$, in the case of low damping at low temperature, the system transfers directly from the disorder locked state to the sliding state of a moving crystal passing the transient plastic-channel regime that at higher damping appears as a truly steady state.

For the higher value of the effective elastic constant, $g_{\text{eff}}=0.257$, at the low temperature the scenario of the ordering transition remains essentially the same. The difference with respect to the lower values of g_{eff} is more pronounced at higher damping. While at the low damping only the structure of the channels in the plastic flow regime is changed, at the higher value of damping a new intermediate TJ-like plastic phase emerges at the beginning of the transition prior to the plastic-channel steady state.

For the stiff atomic layer, $g_{\text{eff}}=0.857$, the system passes during the ordering transition through different intermediate

disorder flow regimes. We observed two plateaus on the $B(F)$ dependence. The first steady state corresponds to a disordered TJ plastic phase with the immobile atoms in the sea of sliding atoms with low mobility. When driving force increases, the system transfers to the state of a moving crystal where, contrary to the case of soft systems, the atomic motion inside the rows is arranged in a solitonlike fashion. For higher damping, a new intermediate solitonic phase emerges prior to the elastic (crystalline) flow of particles. At this stage we observed a formation of moving antikinks inside the rows. These kinks form perpendicularly oriented domain walls which move in the direction opposite to the external driver.

At higher temperature, the depinning force decreases and the drift of atoms starts from a sea of thermally fluctuating particles. While for the stiff atomic layer the scenario of the transition remains almost the same, for the soft system and at the higher value of damping, the plastic channel flow regime that existed at low temperature is destroyed. When driving force increases, the system transfers first from the locked state to the disordered TJ plastic regime and then to the sliding crystalline phase.

When the system is overdamped, the lattice can depin only in the case of strong interatomic interaction ($g_{\text{eff}}=0.857$). For the soft atomic layer ($g_{\text{eff}}\ll 1$), the mobility remains at a low level even at the high value of the driving force ($F\approx 0.8$). We observed the transition from the locked state to the disorder TJ plastic flow which retains this structure even at very high driving force. Thus, our results for the $\theta=0.75$ case are in agreement with previous studies [26,27] and confirm that in the overdamped system at incommensurate concentrations the motion is plastic at high driving.

Although we have considered only one value of the concentration, our results should be qualitatively valid for a general case of incommensurate systems with $0.5 < \theta < 1$. While the studies of the overdamped motion have applications in such areas as dynamics of vortex lattices, charged density waves, colloidal suspensions, and magnetic bubble arrays, where already a lot of experimental works have been done, the studies of underdamped motion are of great importance for tribology [9,41,42]. The studies of the mechanism of the locked-to-sliding transition could give a great contribution to understanding the phenomena of friction and lubrication between two flat macroscopic surfaces on atomic scale. Since solid-state physicists and chemists have only recently begun to study the microscopic friction, new experiments and theoretical approaches are needed in order to complete these studies.

ACKNOWLEDGMENTS

This research was supported in part by the Hong Kong Research Grants Council (RGC) and the Hong Kong Baptist University Faculty Research Grant (FRG). O.B. was partially supported by the NATO Collaborative Linkage Grant No. PST.CGL.980044.

- [1] G. Blatter *et al.*, Rev. Mod. Phys. **66**, 1125 (1994).
- [2] M. J. Higgins and S. Bhattacharya, Phys. Rev. Lett. **74**, 3029 (1995).
- [3] G. Grüner, Rev. Mod. Phys. **60**, 1129 (1988).
- [4] C. Reichhardt and C. J. Olson Reichhardt, Phys. Rev. Lett. **92**, 108301 (2004).
- [5] C. Reichhardt, C. J. Olson, N. Grønbech-Jensen, and F. Nori, Phys. Rev. Lett. **86**, 4354 (2001).
- [6] A. A. Middleton and N. S. Wingreen, Phys. Rev. Lett. **71**, 3198 (1993).
- [7] C. Reichhardt and C. J. Olson Reichhardt, Phys. Rev. Lett. **90**, 046802 (2003).
- [8] R. Seshadri and R. M. Westervelt, Phys. Rev. B **46**, 5150 (1992).
- [9] B. N. J. Persson, *Sliding Friction: Physical Principles and Applications* (Springer-Verlag, Berlin, 1998); Surf. Sci. Rep. **33**, 83 (1999).
- [10] D. Cule and T. Hwa, Phys. Rev. Lett. **77**, 278 (1996); Phys. Rev. B **57**, 8235 (1998).
- [11] A. I. Larkin and Yu. N. Ovchinnikov, Zh. Eksp. Teor. Fiz. **65**, 1704 (1973) [Sov. Phys. JETP **38**, 854 (1974)].
- [12] E. H. Brandt, Phys. Lett. **77A**, 484 (1980).
- [13] J. B. Sokoloff, Phys. Rev. Lett. **86**, 3312 (2001); Phys. Rev. B **65**, 115415 (2002).
- [14] V. M. Vinokur, M. C. Marchetti, and L.-W. Chen, Phys. Rev. Lett. **77**, 1845 (1996).
- [15] H. J. Jensen, A. Brass, and A. J. Berlinsky, Phys. Rev. Lett. **60**, 1676 (1988); A. Brass, H. J. Jensen, and A. J. Berlinsky, Phys. Rev. B **39**, 102 (1989); H. J. Jensen, Y. Brechet, and A. Brass, J. Low Temp. Phys. **74**, 293 (1989).
- [16] H. J. Jensen, in *Phase Transitions and Relaxation in Systems with Competing Energy Scales*, edited by T. Riste and D. Scherrington (Kluwer, Dordrecht, 1993), p. 129.
- [17] R. Besseling, R. Niggebrugge, and P. H. Kes, Phys. Rev. Lett. **82**, 3144 (1999).
- [18] A. E. Koshelev and V. M. Vinokur, Phys. Rev. Lett. **73**, 3580 (1994).
- [19] V. M. Vinokur and T. Nattermann, Phys. Rev. Lett. **79**, 3471 (1997).
- [20] T. Giamarchi and P. Le Doussal, Phys. Rev. Lett. **76**, 3408 (1996); Phys. Rev. B **57**, 11 356 (1998).
- [21] K. Moon, R. T. Scalettar, and G. T. Zimanyi, Phys. Rev. Lett. **77**, 2778 (1996).
- [22] U. Yaron *et al.*, Nature (London) **376**, 753 (1995).
- [23] F. Pardo *et al.*, Nature (London) **396**, 348 (1997).
- [24] G. D'Anna *et al.*, Phys. Rev. Lett. **75**, 3521 (1995); T. Tsuboi *et al.*, *ibid.* **80**, 4550 (1998).
- [25] C. J. Olson, C. Reichhardt, and F. Nori, Phys. Rev. Lett. **81**, 3757 (1998).
- [26] C. Reichhardt and F. Nori, Phys. Rev. Lett. **78**, 2648 (1997); C. Reichhardt, C. J. Olson, and F. Nori, Phys. Rev. B **58**, 6534 (1998).
- [27] C. Reichhardt and N. Grønbech-Jensen, Phys. Rev. B **63**, 054510 (2001).
- [28] C. Reichhardt, G. T. Zimanyi, and N. Grønbech-Jensen, Phys. Rev. B **64**, 014501 (2001).
- [29] C. Reichhardt, G. T. Zimanyi, R. T. Scalettar, A. Hoffmann, and I. K. Schuller, Phys. Rev. B **64**, 052503 (2001).
- [30] C. Reichhardt and C. J. Olson Reichhardt, e-print cond-mat/0311489.
- [31] C. Reichhardt and F. Nori, Phys. Rev. Lett. **89**, 024101 (2002).
- [32] O. M. Braun and Yu. S. Kivshar, *The Frenkel-Kontorova Model* (Springer, Berlin, 2004); Phys. Rep. **306**, 1 (1998).
- [33] O. M. Braun, A. R. Bishop, and J. Röder, Phys. Rev. Lett. **79**, 3692 (1997).
- [34] O. M. Braun, T. Dauxois, M. V. Paliy, and M. Peyrard, Phys. Rev. Lett. **78**, 1295 (1997).
- [35] M. Paliy, O. Braun, T. Dauxois, and B. Hu, Phys. Rev. E **56**, 4025 (1997).
- [36] O. M. Braun, B. Hu, A. Filippov, and A. Zeltser, Phys. Rev. E **58**, 1311 (1998).
- [37] O. M. Braun, B. Hu, and A. Zeltser, Phys. Rev. E **62**, 4235 (2000).
- [38] O. M. Braun, H. Zhang, B. Hu, and J. Tekic, Phys. Rev. E **67**, 066602 (2003).
- [39] O. M. Braun, M. V. Paliy, J. Röder, and A. R. Bishop, Phys. Rev. E **63**, 036129 (2001).
- [40] O. M. Braun, T. Dauxois, M. V. Paliy, and M. Peyrard, Phys. Rev. E **55**, 3598 (1997).
- [41] O. M. Braun, A. R. Bishop, and J. Röder, Phys. Rev. Lett. **82**, 3097 (1999).
- [42] O. M. Braun and M. Peyrard, Phys. Rev. E **63**, 046110 (2001).
- [43] O. M. Braun and V. K. Medvedev, Usp. Fiz. Nauk **157**, 631 (1989) [Sov. Phys. Usp. **32**, 328 (1989)].
- [44] W. Humphrey, A. Dalke, and K. Schulten, J. Mol. Graphics **14**, 33 (1996); <http://www.ks.uiuc.edu/Research/vmd/>
- [45] Movies illustrating different regimes are available at <http://www.iop.kiev.ua/~obtraun/fj-2d.htm>